

A METHOD FOR CHANGE DETECTION WITH MULTI-TEMPORAL SATELLITE IMAGES USING THE RX ALGORITHM

J. A. Malpica* and M. C. Alonso

Dept. of Mathematics, Alcala University, Escuela Politecnica, 28871 Madrid Spain - (josea.malpica, mconcepcion.alonso)@uah.es

KEY WORDS: Change detection, SPOT5 imagery, RX algorithm, anomaly detection, outlier detection, high-resolution satellite image

ABSTRACT:

The use of new, high-resolution spectral sensors, in contrast with low-resolution, increases both the amount of information acquired about land cover at local scales, and the geometric detail and accuracy. However, the algorithms needed for high-resolution image processing are more complex than those needed for their low-resolution counterparts. This paper's main objective is to present a new method for change detection for bi-temporal, multi-spectral, high-resolution satellite imagery. The method focuses on detecting anomalies in two images with the RX algorithm, and then analysing the differences. As a case study, the method is tested with two SPOT5 satellite images pansharpened to a resolution of 2.5 m. Most of the changes that happened to manmade objects between the two dates are obtained by this method.

1. INTRODUCTION

Many algorithms and techniques have been proposed in the last two decades for change detection using multi-temporal satellite data; the most popular techniques are based on algebraic operations, transformations, classification, neural networks, etc.; see a review by Lu et al. (2004). Low-resolution satellite imagery commonly uses pixel-by-pixel change detection methods. This cannot be applied to high-resolution satellite imagery (i.e. SPOT5), due to the complexity of the scene; these images have greater detail, with many new signatures from different materials appearing in high-resolution images that were not detected in low-resolution images. For example, shadows present a problem in high-resolution imagery but not low-resolution imagery. We discuss SPOT5 imagery here, but other satellites have even higher resolution, and the change detection method presented here could be applied with the proper modifications. These satellites include Ikonos, Quickbird, WorldView-1 and many more to be launched in the near future; among them, the WorldView-2, scheduled for launch in 2009, will provide eight-band multispectral imagery for mapping and monitoring applications. It will offer a ground resolution of 0.5 m panchromatic and 1.6 m multispectral. These high-resolution satellite images offer significant cost savings compared to aerial photography as a result of the larger footprints, which means that less ground control and less processing are necessary for orthorectification. High-resolution satellites have more frequent revisit times than aerial surveys, and therefore there is the potential for automatic feature change detection. The gap between aerial photography and satellite imagery is progressively being bridged. One proof of this is national map agencies show increasing interest in this type of imagery; they are acquiring it frequently. This imagery is very useful for change detection of manmade objects, and especially in suburban and urban areas, but most of this work is being done manually. Data from high-resolution sensors clearly offer exciting new challenges and opportunities for researching semi-

automatic techniques that could help people working in the cartographic industry.

2. DATA CHARACTERISTICS AND PREPROCESSING

To see the method's potential, two images from the SPOT5 satellite have been used. The SPOT5 satellite was launched in 2002 and captures panchromatic images with a resolution of 2.5 m, and multi-spectral images with a resolution of 10 m. The first image was taken at 9:30 a.m. on 7-24-05 and the second at 11:20 a.m. on 8-12-06; both are of the same area southeast of Madrid, Spain, on a mostly flat terrain. Azimuth and elevation of the sun were (138.03, 64.97) and (150.07, 62.37), respectively.

Even though both images were taken in the summer and with similar azimuth and elevation of the sun, we applied a radiometric normalisation to both images in order to obtain the closest possible brightness conditions between the images. The normalisation we have applied is called multivariate alteration detection (Canty, 2007).

We took 20 control points (with less than 1 m RMS) uniformly distributed throughout the study area. A subset of the control points were chosen and were subsequently used as independent checkpoints. These were also distributed approximately uniformly. With the metadata from the SPOT5 satellite, the control points and a DEM (5 m resolution) acquired from the Spanish National Map Agency (Instituto Geográfico Nacional, IGN), we orthorectified both images. Then we applied PCA pansharpening to both images in order to obtain two images with four multispectral bands, with 2.5 m resolution each. Then both images were co-registered until errors were under one pixel.

* Corresponding author.

3. ANOMALY DETECTION AND THE RX ALGORITHM

The objective of anomaly detection in multispectral and hyperspectral images is to find pixels that are significantly different from the majority of the pixels in the image.

The RX algorithm was developed by Reed and Yu (1990) (and is named for its authors Reed and (Xiaoli) Yu); and it is given by the equation:

$$\delta(\vec{x}) = (\vec{x} - \vec{m})^T \Sigma^{-1} (\vec{x} - \vec{m}) \quad (1)$$

where \vec{x} = vector representing the pixel
 \vec{m} = mean of surrounding pixels of \vec{x}
 Σ = covariance matrix
 T = transpose

Equation (1) is in fact the Mahalanobis distance. The RX algorithm is a local anomaly detector, which means it generally considers only the surrounding pixels to determine the nature of a pixel. We are going to use RX as a global anomaly detector evaluating each pixel in comparison to the entire window image under study (as the ones shown in Figure 1 and Figure 2).

There are many other alternatives to find anomalous pixels; for example, using the lower components (Sanz et al., 2007), and using projection pursuit with the Lagrange index (method to be published somewhere else by the authors). There are also improvements or generalizations of the RX algorithm, for example the one called the kernel RX-algorithm, which is a nonlinear version of the RX (Kwon and Nasrabadi, 2005).

Although we attempted other anomaly detector approaches, we found that the local R-X algorithm consistently worked well for the imagery analysed. Eventually we are going to compare the bitemporal images; and we found that the extra computational time the generalize methods needed over the most popular RX was not worth it.

RX detects the outliers in the pixel distribution, or what is the same, the anomalies in the images. In this paper, outliers and anomalies are going to be synonymous, despite the statistical and image analysis connotation for the former and the latter, respectively.

Our approach is close to that of Carlotto (2005) who presents a method for object and change detection that first clusters the images and then analyses the distribution of pixel values within clusters over the images. The advantage of clustering is that the misregistration on the images does not affect the change detection.

4. RESULTS AND DISCUSSION

Our first application experiment was carried out on two images of Alcala university campus (Figure 1). The first was taken from 2005 SPOT5 imagery (a) and the second from 2006 (b). A few changes between both dates can be observed visually; for example in the upper right corner of the images a new building was constructed in this period; this corresponds to a new

technological campus for the university. Also, some work was going on at the sport facilities in 2005 that was completed in 2006, etc.

Figure 1 (c) and Figure 1 (d) are the results of applying the RX algorithm to the images of Figure 1 (a) and Figure 1 (b), respectively.

The subtraction of the images in Figure 1 (c) and Figure 1 (d) yields the image in Figure 1 (f). The change-detection image of Figure 1 (f) summarizes many of the 2005-06 changes in one image. The brighter pixels identify positive changes (first image general state brightness was greater than the second image state brightness), while dimmer pixels identify negative changes (initial image brightness was less than second image brightness). Therefore, it shows both types of changes in brightness values; the brighter the value, the more evidence we have about a positive change and the dimmer the pixel, the more evidence for a negative change. The images on the left Figure 1 (e) and on the right Figure 1 (g) of Figure 1 (f) represent the extreme values for the positive and negative changes, respectively. They have been obtained with thresholds in the histogram of Figure 1 (f), the positives for value 1 and the negatives for value 255 (and inverting the digital values of the image in order to obtain a white background).

As can be observed, the algorithm has detected most of the man-made changes such as the new buildings in the upper right and also a new rectangular building on the bottom right corner. Much of the land in the upper left corner has been also been detected as change; this makes sense according to the conceptual characteristics of the algorithm. The RX algorithm looks for outliers, and the piece of land in the upper left corner of image Figure 1 (b) is relatively small compared to the whole image and with a very different spectral characteristic.

In these false-colour images, photosynthesizing vegetation always adds a red tint; in this way, the most intense vegetation areas appear with bright red colours. They are more common in Figure 1 than in Figure 2. This type of vegetation is considered an anomaly in the latter more than in the former. This is the case with the rugby court in the upper centre of the image in Figure 1, which is detected only to a certain degree, as can be seen in Figure 1 (e) (f) and (g). On the contrary, the plot with grass in the upper left corner of Figure 2 was detected by the RX algorithm because in this case, photosynthesizing vegetation could be considered rare or anomalous for Figure 2.

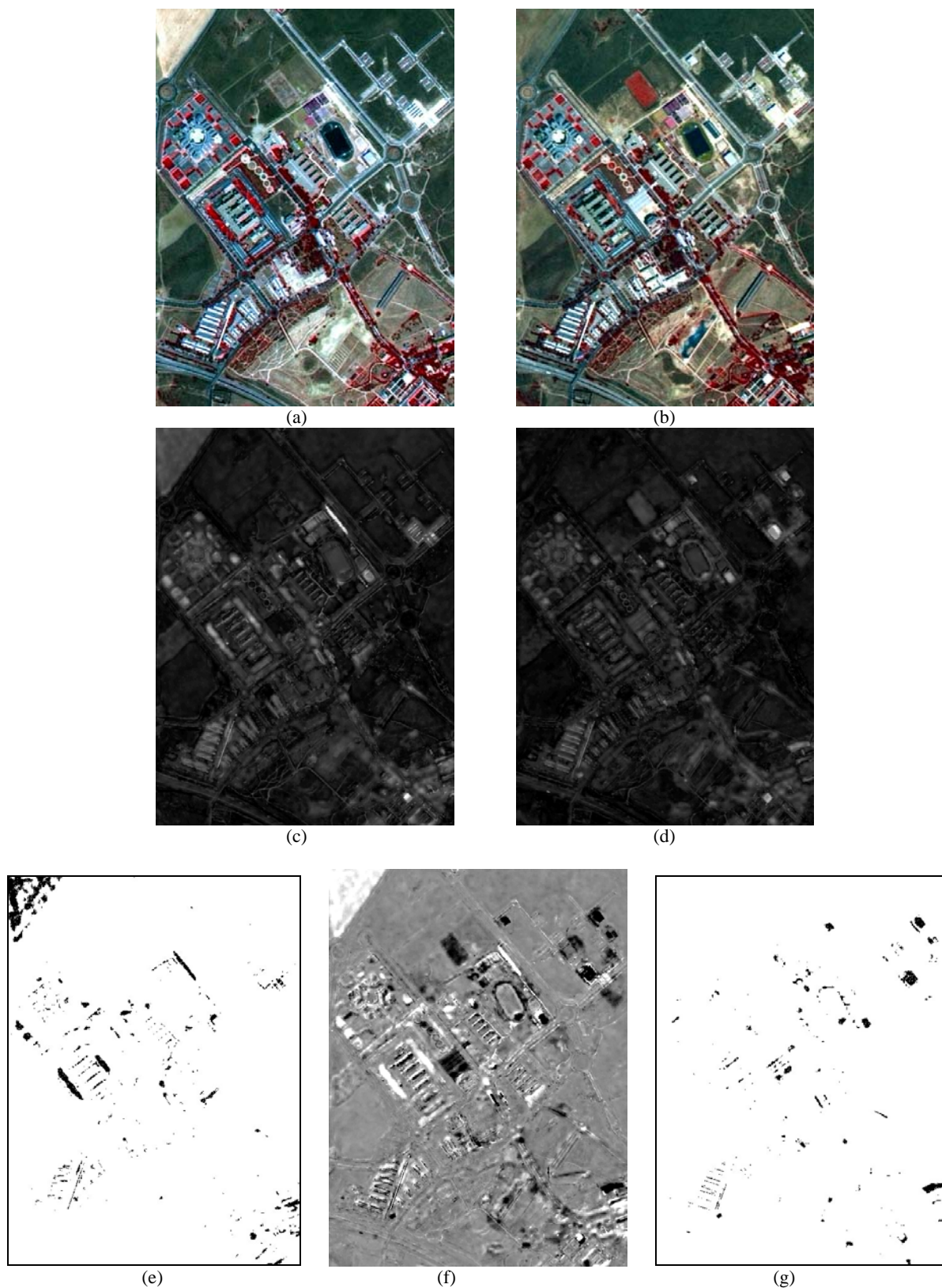


Figure 1. Bitemporal image from Alcalá University campus. (a) Pansharpening SPOT5 for 2005, (b) Pansharpening SPOT5 for 2006, (c) RX algorithm for 2005 image, (d) RX algorithm for 2006, (f) RX image subtraction, 2005 minus 2006. (e) and (g) are the thresholded images of (f) for 1 and 255 digital values respectively.

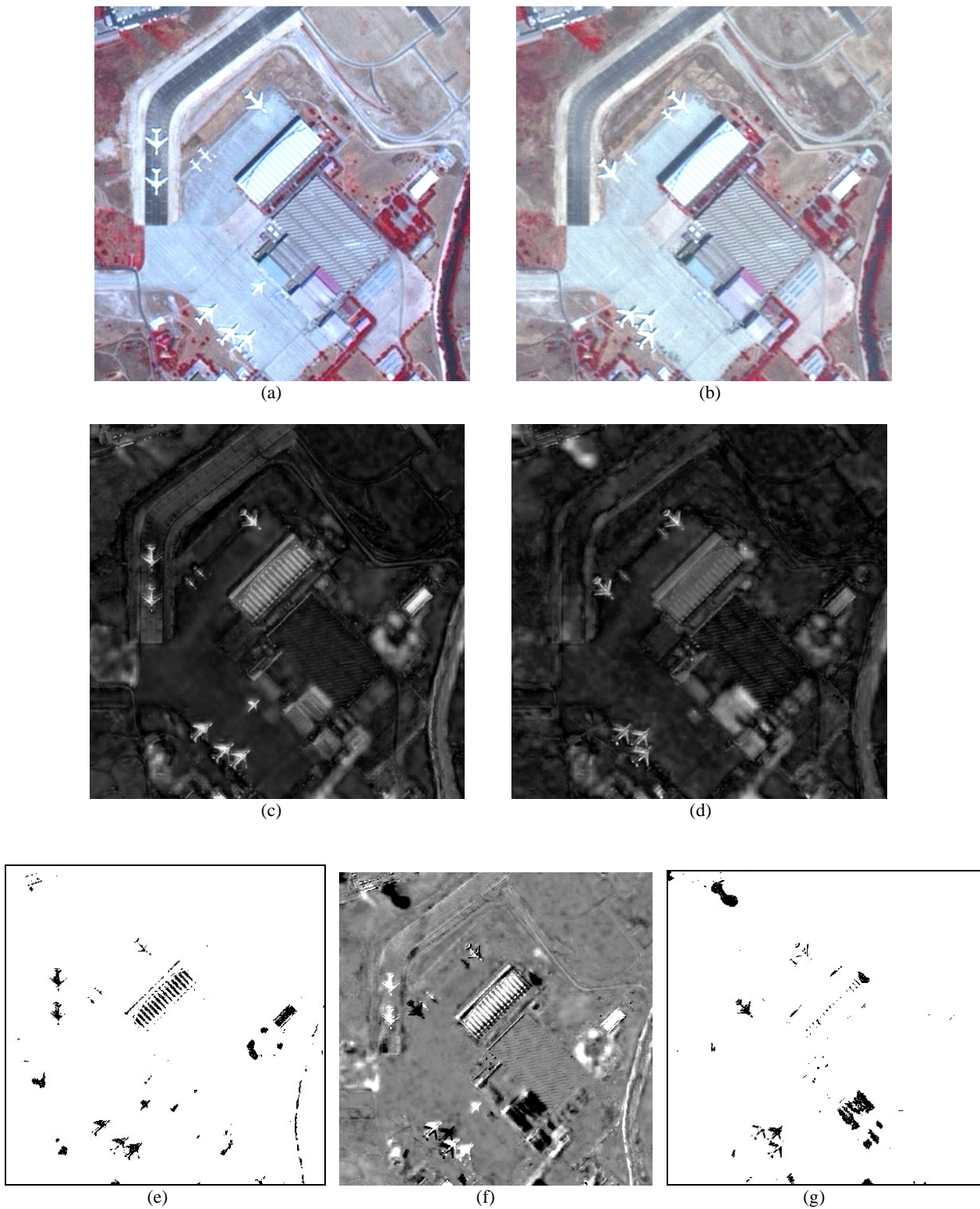


Figure 2. Bitemporal scene from Madrid airport. (a) Pansharpener SPOT5 for 2005, (b) Pansharpener SPOT5 for 2006, (c) RX algorithm for 2005 image, (d) RX algorithm for 2006, (f) RX image subtraction, 2005 minus 2006. (e) and (g) are the thresholded images of (f) for 1 and 255 digital values respectively.

It is interesting that the pond, empty in Figure 1 (a), and full in Figure 1 (b) has not been detected as a clear change. This is due to the spectral characteristics of water, which are similar to other spectra in the image and does not result as an anomalous

spectral in the image. Water appears almost black because at this angle, it scatters little light back to the SPOT5 sensor.

Construction land appears brighter; bulldozed soil, bare of vegetation, is very reflective. See the construction work Figure

1 (a) in the sport facilities and the technical campus on the upper right. This is very convenient for change detection with the RX approach.

Another two sub-images were taken from the 2005-06 SPOT5 imagery. This time we cut an image representing an area of Madrid Barajas airport. The experiment was carried out in the same way as the Figure 1 pair of images. On the one hand, the airplanes are clearly detected, even the small ones. In the airplanes detected at the bottom of Figure 2 (f) we can see they were not parked exactly in the same place in 2005 and in 2006. On the other hand, the buildings in the centre of the image and in the centre right are detected as changes but they are not. This is due to the difference of reflectance in 2005 and in 2006. The difference in the altitude of the sun in 2005 compared to 2006 is enough to give a big difference in brightness. This is so because of the metallic composition of the roof and its inclination with respect to the horizontal plane.

It is difficult to make an accuracy assessment for the approach presented here. First it would be necessary to define clearly when we consider a change has happened. Nevertheless, most of the manmade objects are detected in both images (Figures 1 and 2): buildings, airplanes, parking lots, etc. Post-classification editing is done to correct some "salt and pepper" effect to isolate areas of significant change.

5. CONCLUSIONS

The technique presented here was based essentially on applying the RX algorithm to two bitemporal images in order to obtain the anomalies for each image. That an anomaly appears in one of the images and not in the other was taken as a change. Our approach is supposed to be a first step in the analysis of the change detection process; once a change has happened it will need further investigation by other means: whether visually by an image analyst or by additional automatic processes.

A great variety of objects were detected whenever their spectral signatures deviated sufficiently from the background. Because most of these images' pixels represent natural materials, the anomalies are represented mostly by artificial objects. The whole anomaly detection process proves to be automatic in the sense that it does not require parameter tuning.

Different change detection algorithms have their own strong points and no single approach can be considered the best for all cases. In practice, different algorithms are often compared to find the optimal change detection algorithm for a specific application. The algorithm proposed in this paper is going to be useful when image analysts are looking for manmade change detection in high-resolution satellite images similar to SPOT5.

Future work remains to be done in normalization. Only a small difference in the sun azimuth and altitude was enough to create big differences in reflectance between the same roofs, and this is the main cause of false alarms.

Most anomaly detection methods suffer from limited performance in the form of excessive false alarm rates. The same problem limits the accuracy of our RX approach. To cut down on false alarms, the approach here presented should be followed by some form of spatial processing. If the number of contiguous pixels expected to cover a given target shape is known, then a similar grouping of detections may also be used as a criterion for target definition. For example, the new

buildings in Figure 1 could be defined as rectangular shapes or the airplanes in Figure 2 as some kind of cross shape.

REFERENCES

- Canty, M.J., 2007. *Image analysis, classification and change detection in remote sensing* Taylor & Francis. Boca Raton, USA pp. 233-257.
- Carlotto, M.J., 2005. A Cluster-Based Approach for Detecting Man-Made Objects and Changes in Imagery. *IEEE Transactions on Geoscience and Remote Sensing*, 43(2), pp. 374-387.
- Lu, D., Mausel, P., Brondizios, E., Moran, E., 2004. Change detection techniques. *International Journal of Remote Sensing*, 25, pp. 2365-2407.
- Kwon H., Nasrabadi, N.M., 2005. Kernel RX-algorithm: a nonlinear anomaly detector for hyperspectral imagery. *IEEE Transactions on Geoscience and Remote Sensing*, 43(2), pp. 388 – 397.
- Reed I. S. and X. Yu, 1990. Adaptive multiple-band CFAR detection of an optical pattern with unknown spectral distribution. *IEEE Transactions on Acoustics, Speech and Signal Processing*, 38, pp. 1760—1770.
- Sanz A., M. C. Alonso y J. A. Malpica. 2007 El Análisis de Componentes Principales y su inverso aplicado a imágenes satelitales de alta resolución. *Topografía y cartografía: Revista del Ilustre Colegio Oficial de Ingenieros Técnicos en Topografía*, 24(142), pp. 42-49.

ACKNOWLEDGEMENTS

The authors wish to thank the Spanish National Mapping Agency (Instituto Geográfico Nacional) for providing the images for this research. The authors are also grateful to the Spanish MCYT for financial support to present this paper; project number CGL2006-07132/BTE.

